

Applied Aerodynamics 085322 Project 2 - Airfoil panel code

Sahar Ben Atar

July 13, 2024

Table of Contents

1.....	Applied Aerodynamics 085322 Project 2 - Airfoil panel code
3.....	Part A - Panel method solver- Hess-Smith model/ Vortex panel method
A.1	The convergence in C_L , C_d , and C_m about the quarter-chord as a function of the
3.....	number of the panels, and the source of the C_d coefficient.
5.....	A.2 discussion about the results between the two panel methods.
8.....	A.3 The differences between the edge type
B.1	A Report for the first three Fourier coefficients (A_0 , A_1 and A_2)- thin airfoil theory
10.....	
11	B.2 C_L and C_m about the quarter-chord as a function of angle of
11	attack- thin airfoil theory
12.....	B.3 C_p distribution- thin airfoil theory
15.....	Appendix, more important graphs.

Part A - Panel method solver- Hess-Smith model/ Vortex panel method

A.1 The convergence in C_l , C_d , and C_m about the quarter-chord as a function of the number of the panels, and the source of the C_d coefficient.

First, let's discuss the methods for calculating the coefficients, where each of them applies?

In the context of potential flow theory and the panel method, the drag coefficient (C_d) is theoretically zero for an inviscid, incompressible flow around a body without separation. This is because potential flow theory assumes an ideal fluid with no viscosity, leading to no shear stresses and thus no skin friction drag. Additionally, for a streamlined body with no separation (according to potential flow theory), there should be no form drag (pressure drag).

However, with surface integration method one can calculate the coefficients by integration of the C_p coefficient. But, during the calculation it can be discovered that the outcome of drag coefficient shows that it is not zero as we expected according to the Potential Flow Theory. The reason for that phenomenon is numerical error, due to discretization of the continuous surface into a finite number of panels that some of them are not in small angles. Which can lead to inaccuracies when C_p get a component at drag direction. Therefore, the drag coefficient outcome is false and doesn't have connection to the real force. That means that the moment coefficient has a small error since it is affected by false drag force.

On the other hand, with Kutta-Joukowski theorem one can calculate the lift and the moment coefficients, without the drag.

For the lift coefficient, the equation is $L' = \rho_\infty U_\infty \Gamma$. where L' is the lift force per unit span, ρ_∞ , U_∞ are the density and the velocity of the free stream, and Γ is the circulation around the airfoil.

Therefore,

$$(1) \quad C_L = \frac{L'}{\frac{1}{2}\rho U_\infty^2 c} = \frac{\rho U_\infty \Gamma}{\frac{1}{2}\rho U_\infty^2 c} = \frac{2\Gamma}{U_\infty c}.$$

And for the moment coefficient, the equation is (2) $C_M = \sum_{i=1}^N C_{L_i} (x_i \cos \alpha)$.

As it can be seen in figure 1, the coefficients get their final value from around $N=80$. Therefore, until that value, there will be a small error due to the approximation of the shape of the airfoil.

In addition, usually it is important not to use many panels. Due to the inverse matrix calculation that needs to be done. If one tries to inverse matrix with high coefficients numbers, it will be too difficult for the computer's memory.

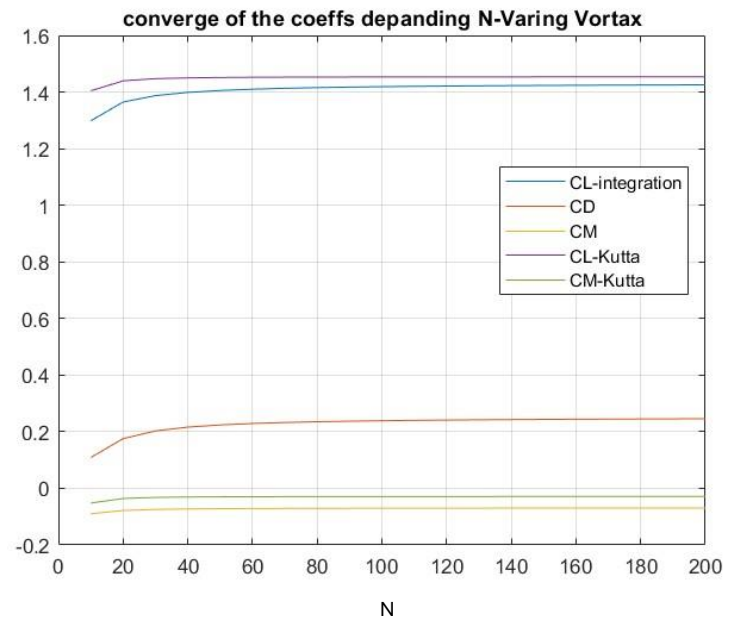
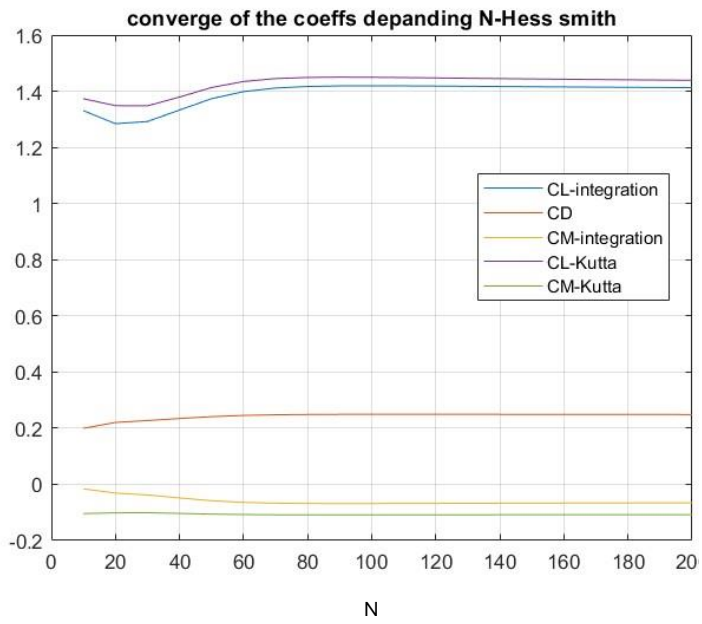


figure1 convergence of coefficients depending on N- using Hess Smith/Varing vprtex methods, at $\alpha=10^\circ$

A.2 discussion about the results between the two panel methods.

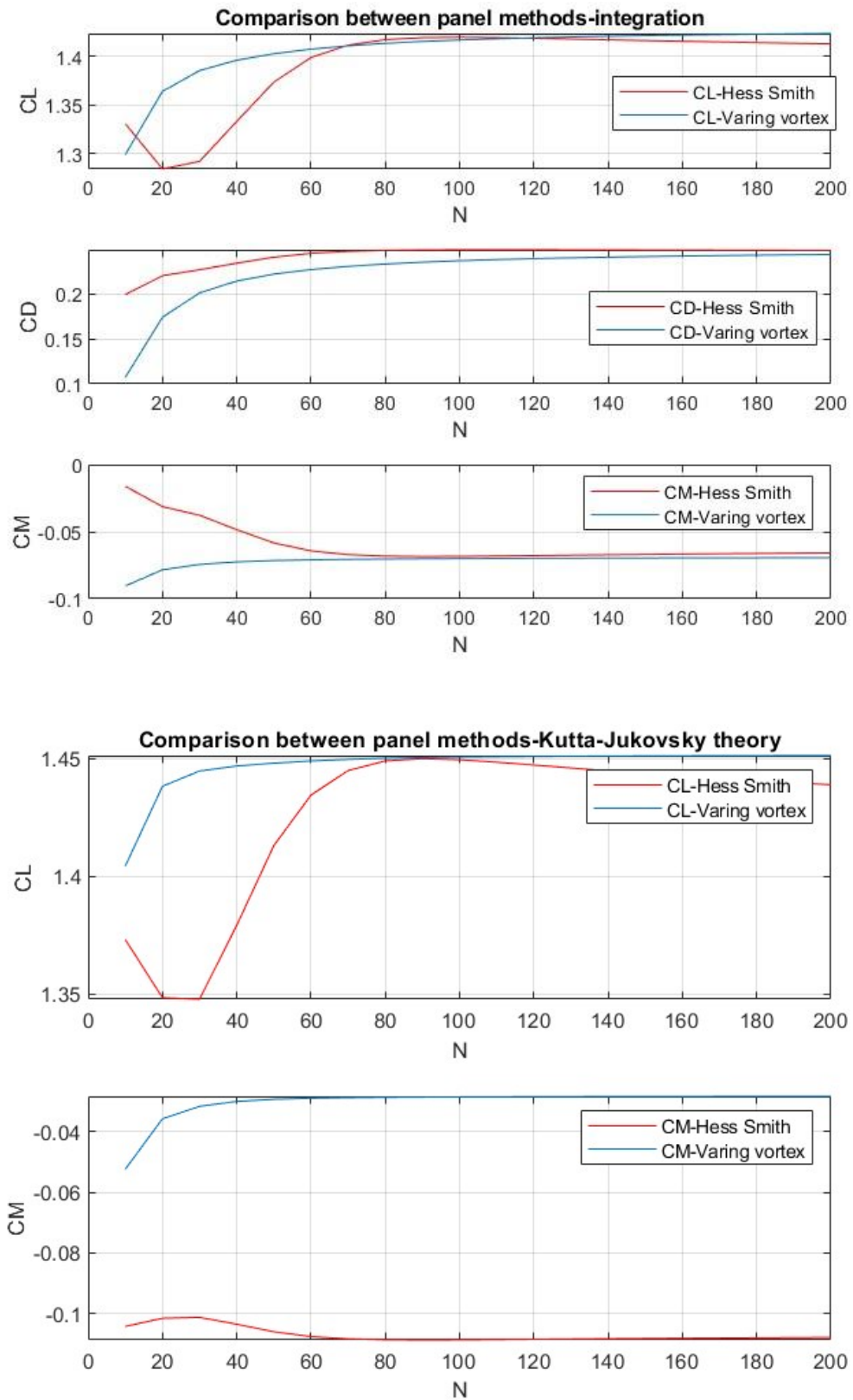


figure 2 comparison between the methods

Comparison between the methods when using surface integration:

The two methods degenerate the closest results when N is around the value of 100.

While the Linear Vortex converges, the Hess-Smith method doesn't.

As well, there is an error in the final value of the C_M coefficient, which caused by the error of C_L .

Let's see the differences when both methods are reliable, at N=100 in the integration case:

$$C_L = 1.4193, C_D = 0.2494, C_M = -0.0684$$

The coefficient values at Linear Varying Vortex N=100:

$$C_L = 1.4166, C_D = 0.2372, C_M = -0.070$$

The two panel methods generate almost the same coefficients with very small errors between each other, when: $\Delta C_L \sim 0.001$ $\Delta C_D \sim \Delta C_M \sim 0.01$. which can be described by numerical errors.

In addition, as can be seen from the graphs, there is another error until the two methods converge at the critical number of panels. This error can be explained with the numeric disturbance that generates since Panel methods discretize the continuous surface into a finite number of panels.

In figure (3) we can see the differences between the C_p distributions:

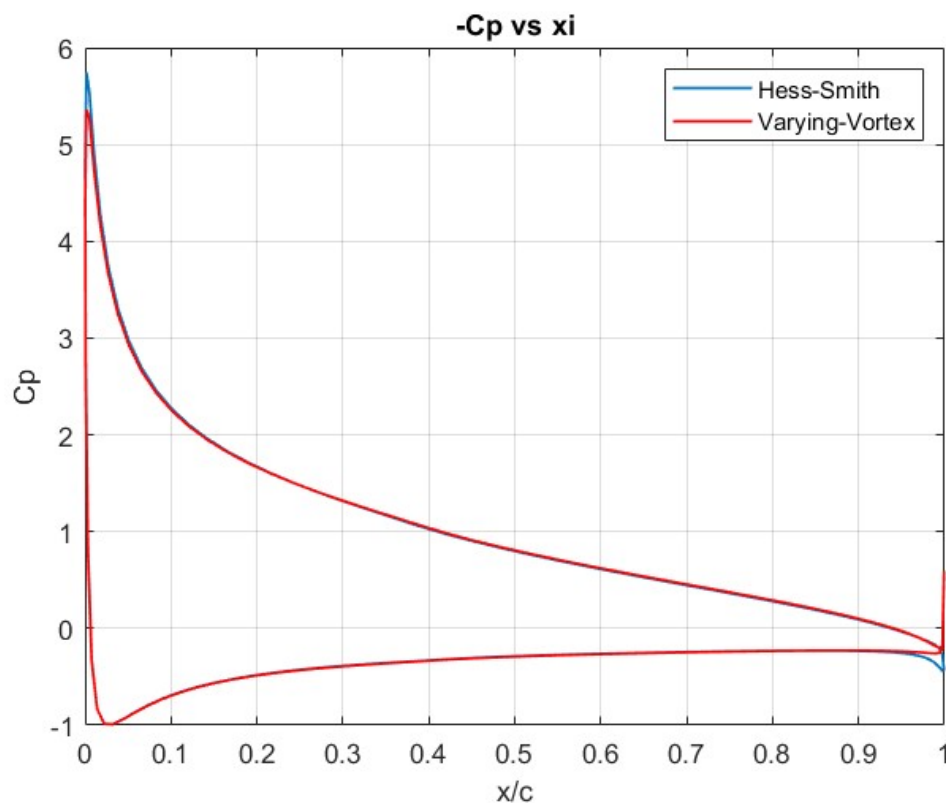


figure 3 comparison between the methods at $\alpha=10[\text{deg}]$, integration case.

As it may be seen, there are differences between the TE of the methods, and between the LE of the methods.

For both differences, they occur since each type of calculations use different technics to calculate. One reason for the gap may be that the Varying-Vortex method uses a linear interpolation between two vortexes, while Hess-smith assume that at each panel the source has constant value. For the error that was responsible for the gap in the TE, the reason may be that the Varying-Vortex method meant to work on sharp edge, but in this question, we asked to calculate with blunt one (more on that will be written in the following question).

A.3 The differences between the edge type

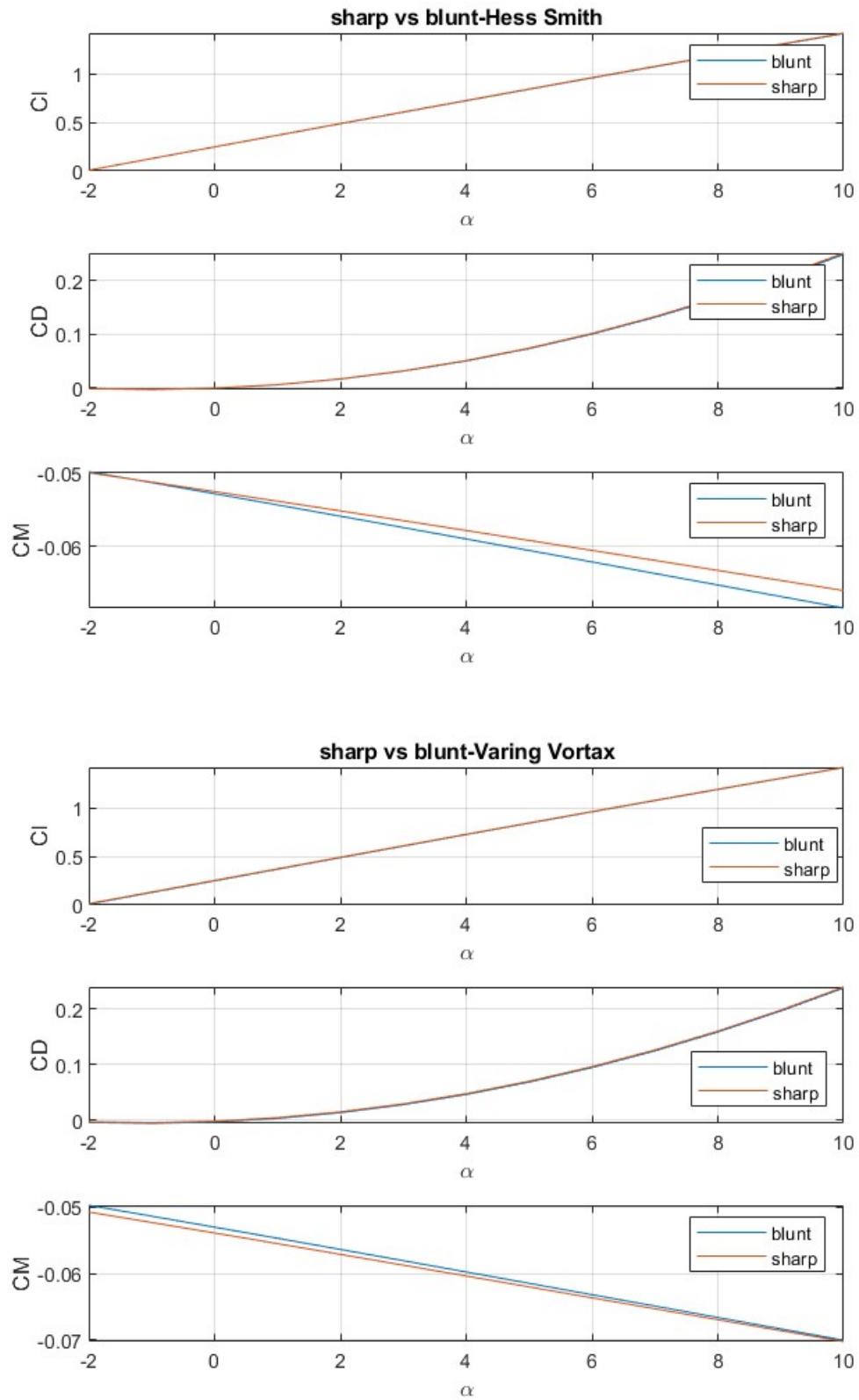


figure4 differences between TE edges

It can be easily seen in figure 3, that the TE type does not affect the coefficient value more than 0.01 at the largest error at C_M .

To make it more clearly, I zoomed in the C_L graph (that appear in the appendix) to see the value of ΔC_L between the sharp and the blunt edge, $\Delta C_L \sim [0.001, 0.005]$, which is depends on the method and the type of calculation.

The largest ΔC_L is when using the Varying Vortex method.

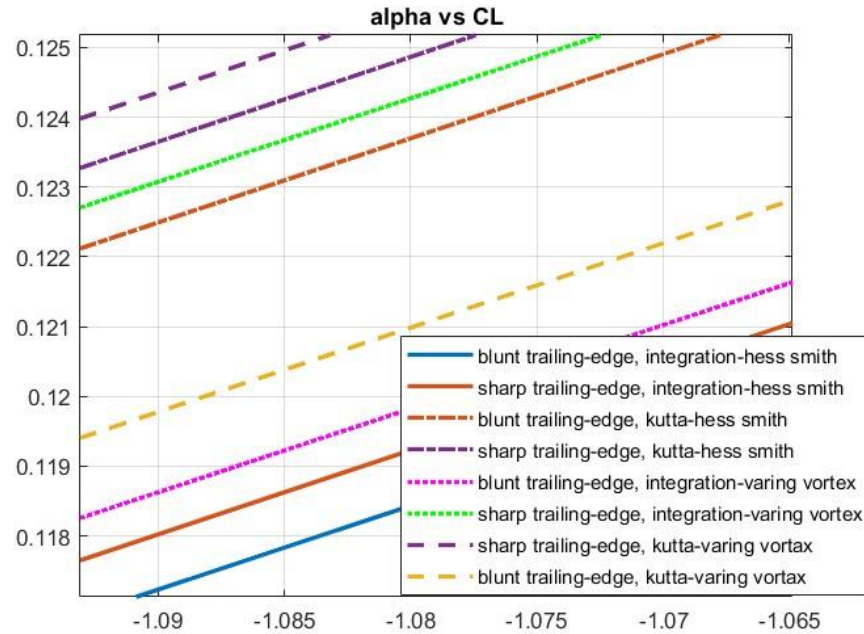


figure 5 zoom in to the C_L coeff

The reason for the large error at Vortex Varying method is since the method was written to calculate airfoils with sharp edges. It is stand up more clearly in figure 5, when the TE has a bend to satisfy the Kutta Condition.

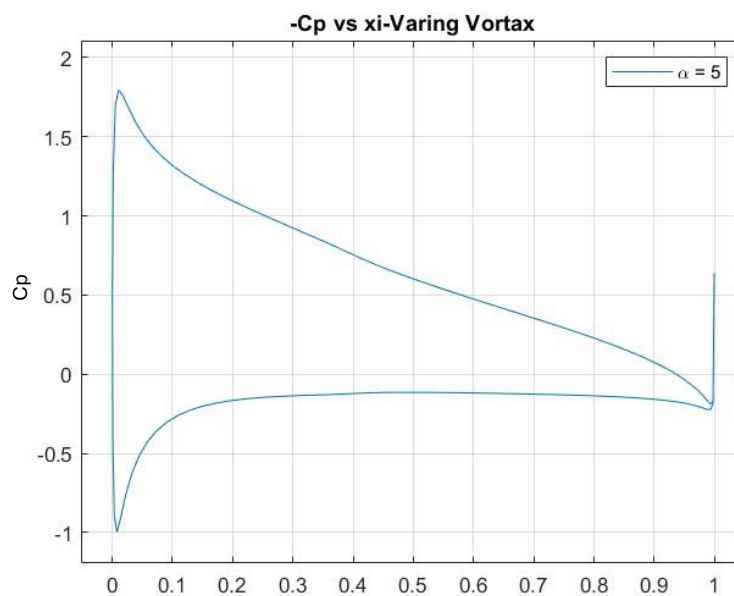


figure 6 C_p distribution for Vortex Varying at $\alpha=5^\circ$

B.1 A Report for the first three Fourier coefficients (A0, A1 and A2)- thin airfoil theory

For that calculation one should use thin airfoil theory on NACA 2412.

In that theory the mean chamber chord of the NACA profile should be used. The formula is given for $(x, y) = \left(\frac{x}{c}, \frac{y}{c}\right)$ meaning that $0 \leq x \leq 1$ which is analog to $c = 1$.

$$(3) \quad \bar{y}(x) = \begin{cases} \frac{m}{p^2} x(2p - x), & 0 \leq x < p \\ \frac{m}{(1-p)^2} (1 - 2p + 2px - x^2) & x \geq p \end{cases}$$

.

Deriving the mean chord function we get:

$$(4) \quad \frac{d\bar{y}(x)}{dx} = \begin{cases} \frac{m}{p^2} (2p - 2x) & 0 \leq x < p \\ \frac{m}{(1-p)^2} (2p - 2x) & x \geq p \end{cases}$$

We define A_n as:

$$(5) \quad \begin{cases} A_0 = \alpha - \frac{1}{\pi} \int_0^\pi \frac{d\bar{y}}{dx}(\theta) d\theta & n = 0 \\ A_n = \frac{2}{\pi} \int_0^\pi \frac{d\bar{y}}{dx}(\theta) \cdot \cos(n\theta) d\theta & n \geq 1 \end{cases}$$

Using the parameter substitution: $x = \frac{c}{2}(1 - \cos\theta)$

Putting the substitution into eq.4

$$(6) \quad \frac{d\bar{y}(\theta)}{dx} = \begin{cases} \frac{m}{p^2} (2p - (1 - \cos\theta)) & 0 \leq \theta < \theta_p \\ \frac{m}{(1-p)^2} (2p - (1 - \cos\theta)) & \theta_p \leq \theta \leq \pi \end{cases}$$

Putting in $m = 0.02, p = 0.4$ for given NACA airfoil

$$(7) \quad \frac{d\bar{y}(\theta)}{dx} = \begin{cases} 0.125(\cos\theta - 0.2) & 0 \leq \theta \leq 1.369 \\ 0.0555(\cos\theta - 0.2) & 1.369 \leq \theta \leq \pi \end{cases}$$

So, the integrals would be:

$$(8) \quad A_0 = \alpha - \frac{1}{\pi} \left[\int_0^{1.369} (0.125 \cos \theta - 0.025) d\theta + \int_{1.369}^{\pi} (0.0555 \cos \theta - 0.011) d\theta \right]$$

Calculating the integral we get:

$$(9) \quad A_0 = \alpha - \frac{1}{\pi} (0.125 \sin(1.369) - 0.025 \cdot 1.369 - 0.011 \cdot (\pi - 1.369) - 0.055 \sin(1.369))$$

And the final value would be:

$$(10) \quad A_0 = \alpha - 0.0047$$

$$(11) \quad A_n = \frac{2}{\pi} \left[\int_0^{1.369} \cos(n\theta) (0.125 \cos \theta - 0.025) d\theta + \int_{1.369}^{\pi} \cos(n\theta) (0.0555 \cos \theta - 0.011) d\theta \right]$$

For A1:

$$(12) \quad A_1 = \frac{2}{\pi} \left[\int_0^{1.369} \cos(\theta) (0.125 \cos \theta - 0.025) d\theta + \int_{1.369}^{\pi} \cos(\theta) (0.0555 \cos \theta - 0.011) d\theta \right]$$

Solving the integral we get:

$$(13) \quad A_1 = 0.0467 + 0.0347 = 0.0814$$

And for A2 similarly:

$$(14) \quad A_2 = \frac{2}{\pi} \left[\int_0^{1.369} \cos(2\theta) (0.125 \cos \theta - 0.025) d\theta + \int_{1.369}^{\pi} \cos(2\theta) (0.0555 \cos \theta - 0.011) d\theta \right]$$

And calculating the integrals we get

$$(15) \quad A_2 = 0.025 - 0.011 = 0.014$$

B.2 Cl and Cm about the quarter-chord as a function of angle of attack- thin airfoil theory

C_l is defined as $C_l = 2\pi \left[A_0 + \frac{A_1}{2} \right]$.

So, using eq.13 and eq.15 the lift coefficient:

$$(16) \quad C_l = 2\pi\alpha + 0.226$$

And for the moment coefficient

$$(17) \quad C_{mac} = \frac{\pi}{4} (A_2 - A_1) = -0.053$$

Therefore, the plot of C_l and C_m as a function of alpha, using MATLAB:

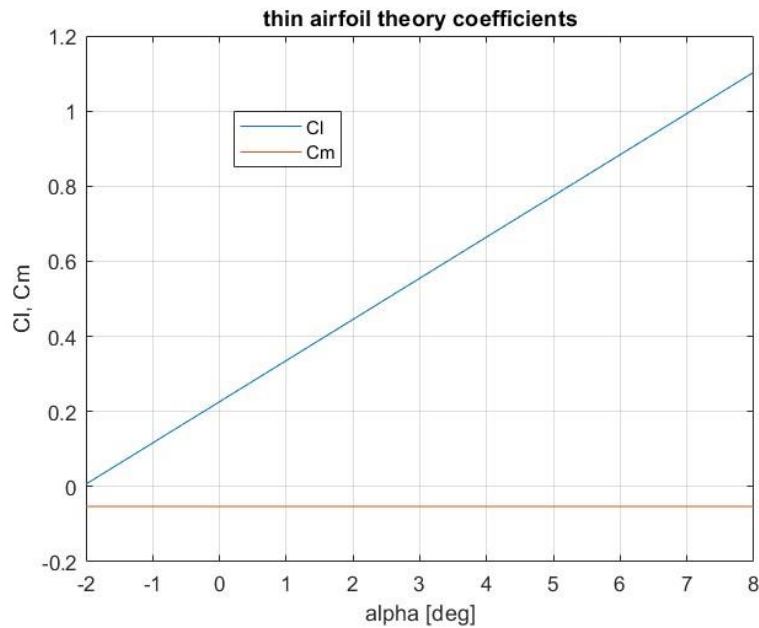


figure 7 thin airfoil theory

B.3 Cp distribution- thin airfoil theory

With assuming small angles $\cos(\alpha) \sim 1$, $\sin(\alpha) \sim \alpha$ and $U_\sigma, U_\gamma \ll V_\infty$ it is possible to make first order approximation for the pressure coefficient.

$$(18) \quad C_p = -2 \frac{U_\sigma + U_\gamma}{V_\infty} = 2 \frac{\gamma(x)}{V_\infty}$$

When:

$$(19) \quad \gamma(x) = 2V_\infty \left[A_0 \frac{1 + \cos(\theta)}{\sin(\theta)} + \sum_{n=1}^{\infty} A_n \sin(n\theta) \right]$$

Putting the equation for finding A_n (eq.5) into MATLAB and demanding a condition of convergence that all the variables of A_n that smaller than 10^{-3} are negligible.

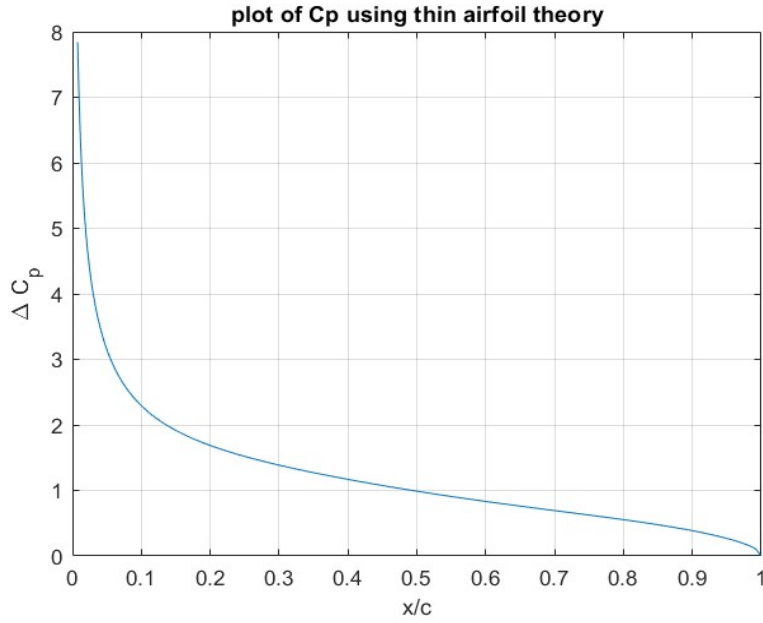


figure 8 Cp distribution, thin airfoil

As it can be seen, the C_p value at the leading edge ($x/c=0$) is diverge. This happens since the component in the equation for finding $\gamma(x)$ (eq.19), $A_0 \frac{1+\cos(\theta)}{\sin(\theta)}$, the value of $\sin(\theta)$

This is happening since thin airfoil theory assumes small disturbances. At the LE that assumption is violated, which leads to the divergence. To fix the divergence at the LE one can use the "Riegel correction".

In addition, it doesn't happen at $\theta = \pi$, since $\gamma(\pi) = 0$ by using L'Hopital's rule.

$$\gamma(\pi) = \lim_{\theta \rightarrow \pi} \gamma(\theta) = 2V_{\infty} \alpha \lim_{\theta \rightarrow \pi} \frac{1 + \cos(\theta)}{\sin(\theta)} = \lim_{\theta \rightarrow \pi} \frac{-\sin(\theta)}{\cos(\theta)} = 0$$

Comparing the panel method results to the thin airfoil one:

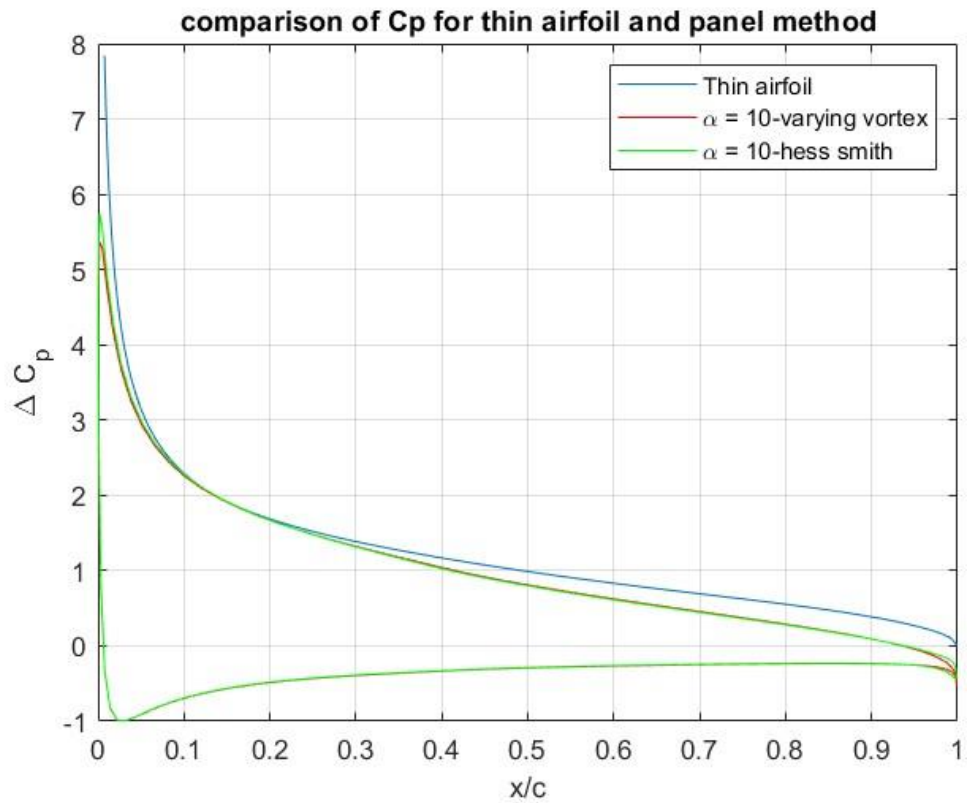


figure 9 comparison between panel method results to the thin airfoil

Both panel methods and thin airfoil theory yield similar results, except for discrepancies at the leading edge and the trailing edge that had been talked about before and another small difference.

This difference arises because thin airfoil theory considers only the mean camber line, while the panel method also accounts for the airfoil's thickness.

Appendix, more important graphs.

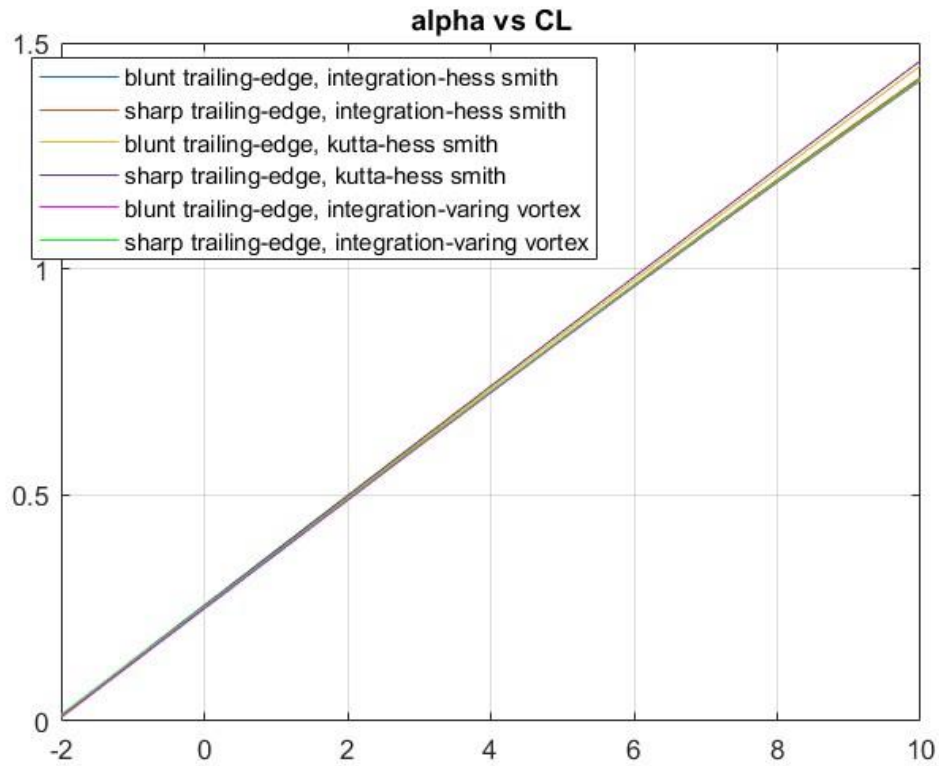


figure 10 CL vs $\alpha[\text{deg}]$

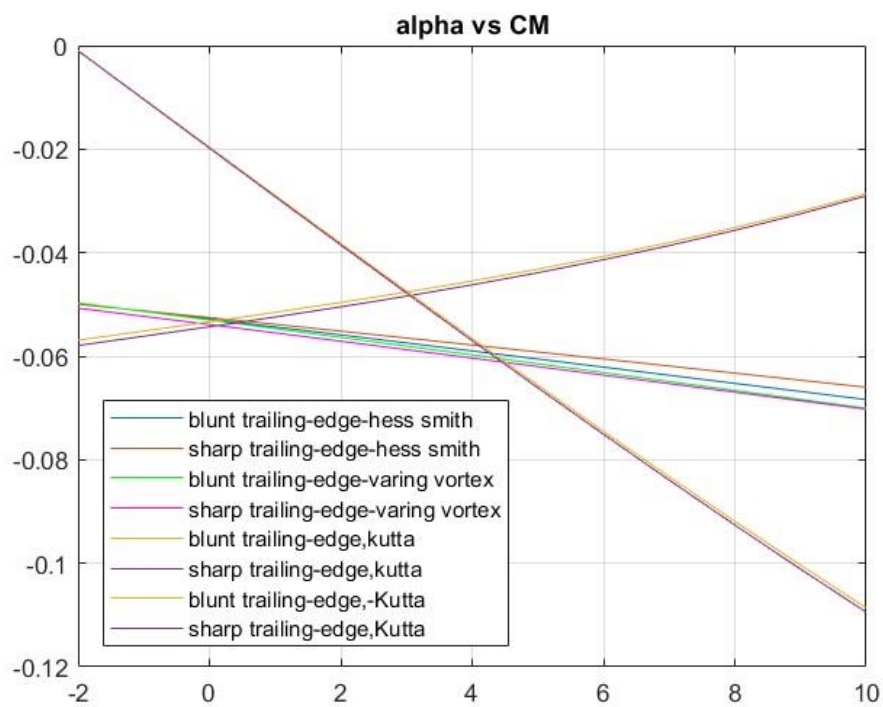


figure 11 C_m vs $\alpha[\text{deg}]$, aproximatly value 0

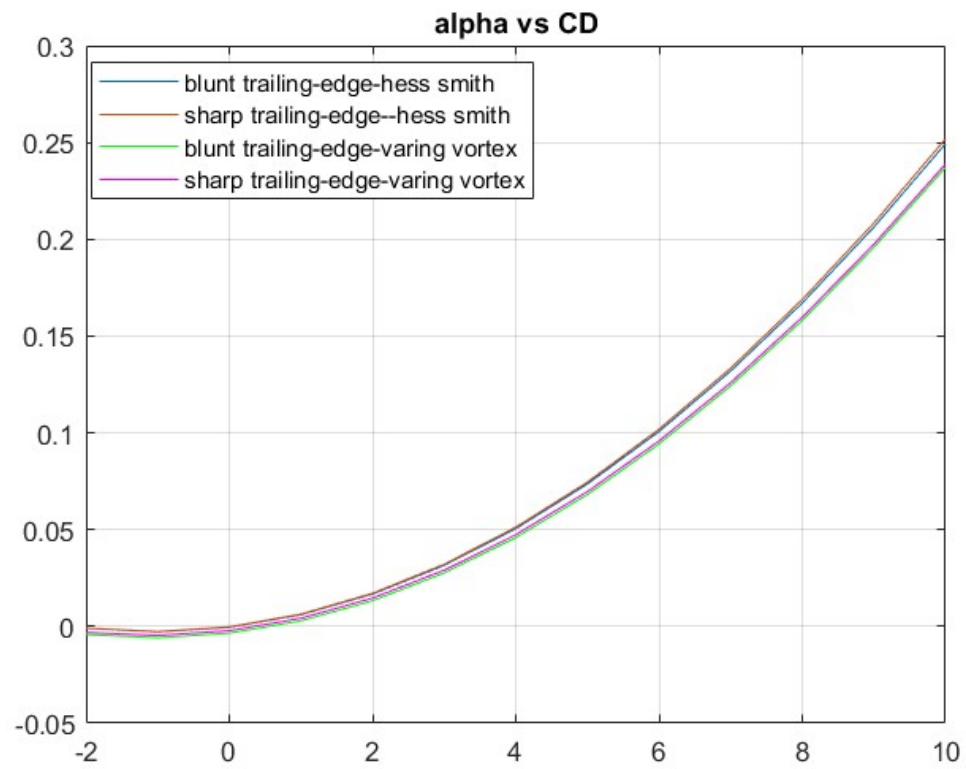


figure 12 alpha vs C_D , not physical, but a numeric error.